Simulation platform for modelling and calibration of hybrid vehicles energy management from experimental input

Cano, Pablo; Roche, Marina; Hernández, Albert; Sabriá, Dídac; Mammetti, Marco

Applus IDIADA, L'Abornar PO Box 20, E-43710 Santa Oliva (Tarragona) Spain

ABSTRACT

Hybridizing vehicles is one of the paths followed by OEM`s to reduce their vehicle consumption and emissions. The premium segment is facing severe problems in reaching European environmental exhaust targets when running on fossil fuel only. The European-funded project, ADVICE, targeted this issue by aiming at increasing the market penetration of hybrid vehicles by cost reduction and by technology improvement. Simulation models are a cost-efficient approach to evaluate the impact of a technology on a variety of driving conditions or to virtually evaluate the impacts of potential improvements.

This paper presents a methodology to generate a reliable hybrid vehicle model exclusively from experimental data and validate it with objective KPIs. The methods we present permit obtaining sufficient components and strategy characterization accuracy from dynamic vehicle-level tests such as WLTP or RDE. The advantage of this methodology is its capability to maximize the outcome of the regular vehicle-level testing activities to generate a predictive vehicle consumption model without the need of specific component or stabilized condition testing. Specific correlation KPIs were applied in order to guarantee adequate correlation between various signals acquired in the experimental and simulated activities. This methodology guarantees the accuracy and predictivity of the models. These models were used to calculate the impact of different improvements in consumption.

1. INTRODUCTION

The European-funded project, ADVICE, had the scope of increasing the market penetration of hybrid vehicles by cost reduction and by technology improvement [1]. This can be achieved lowering the fuel consumption and emissions, maximizing the driving time in full electric mode and improving the performance and efficiency of the main subsystem components in the vehicle.

In the project, three demonstrators were hybridized applying innovations at component, control, and vehicle level. The results of the vehicle-level validation tests were used to illustrate the methodology of predictive consumption model building exclusively from experimental test data. This methodology has proven exploitation interest due to its cost-efficient model generation process, enabling the capability to generate a database of simulation models generated from experimental activities. This database can be used to make a deeper analysis of the experimental activities in order to compare the impact of properties (such as aerodynamic resistance, weight, components efficiency, hybridization level, management strategy…) on fuel consumption or evaluating the impact of applying a best-in-class technology in a certain vehicle. Furthermore, it can be used to predict the vehicle consumption in a wider variety of driving conditions than those that were originally tested in order to evaluate the efficiency on different real use profiles (gentle vs aggressive, urban vs mountain, etc.) and better assess the impact of the technology on its end users as illustrated in [2].

This paper presents the methodology to obtain the components and strategy characterization from the vehicle level test and implement a simulation model that guarantees correlation both with instantaneous and aggregated values in order to ensure predictivity.

2. METHODOLOGY

This section presents the applied methodology that can be extrapolated to further applications, while the following sections present the application to a specific case in the ADVICE project.

The process to generate the model for simulation from experimental data is depicted in Figure 1 and described in the following paragraphs.

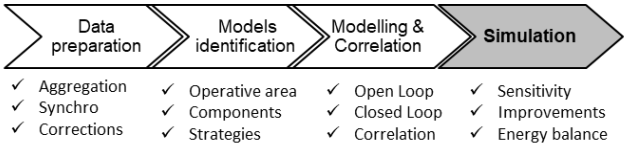

Figure 1. Model generation process.

2.1. DATA PREPARATION. These steps consist of data aggregation from different data sources, namely testing facility recordings, instrumentation recordings and/or signals from vehicle CAN data.

This data aggregation has to be made with caution, because input data is usually desynchronized, noisy, at different sampling rates and subjected to measurement uncertainties or offsets, making it not possible to easily perform model parameters identification from transitory data. For these reasons it is crucial to make proper data preparation filtering, synchronization, and offset correction of tested signals in order to reduce the noise factors that affect the correlation process.

The first step is data synchronization among different data sources, and also among different channels of same data source. Even though all the channels in a data source are recorded synchronously, the measurement process itself may induce a delay (for example, if fuel is measured by the analysis of the composition of exhaust gases, there is a delay from the moment the fuel is consumed to the moment the

gases are measured). Without data synchronization, it is not possible to perform regression on instantaneous signals nor to generate compound signals by aggregation, multiplication, or division. The metric used to evaluate the synchronization between signals, is the cross-correlation [3]:

$$F\{f * g\} = \overline{F\{f\}} * F\{g\} \quad (1)$$

Where f and g are two real value functions, F denotes the calculation of the Fourier transform and $\overline{F\{f\}}$ denotes the complex conjugate. After calculating the cross-correlation between two signals, the maximum or minimum of the cross-correlation function indicates the point in time where the signals are best aligned.

After synchronization, signals are analysed and cross-checked with available signals in order to apply the proper corrections. Figure 2 shows the influencing factor applying to the correlation process [4].

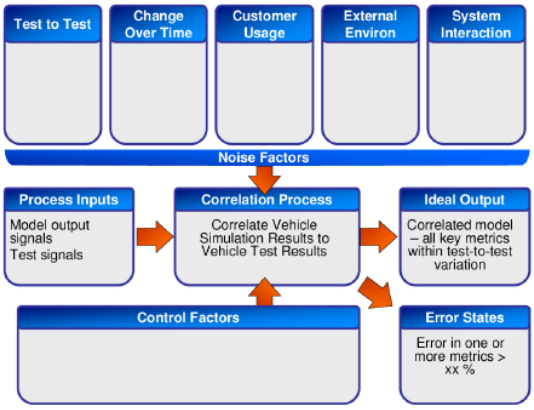

Figure 2. P-Diagram framework for hybrid electric vehicle simulation to test correlation [4].

These corrections may include, among others:

-Proportional deviations: this correction applies for example to the CAN speed that presents a proportional deviation due to the estimation of the wheel radius

-Offsets: constant offsets may apply to sensed signals such as the current. These offsets should be corrected due to their big impact on aggregated-over-time results. Time dependent offsets may also apply because of change over time during the test (e.g. temperature)

-New signal derivation: identification of a new relevant signal from sensed data. This may apply to instantaneous fuel consumption calculation from aggregated and saturated fuel signals, or rpm calculation from encoder signal

-Data filtering & signal loss: this type of data processing applies mostly to high frequency signals and signals derived from GPS positioning (position, speed, slope…)

-The output of this step is an aggregation of pre-processed signals from different sources ready for parameter identification.

2.2. IDENTIFICATION. Model equations and parameter identification is performed with a custom correlation tool. The first step of the process is the analysis of the operative region of each of the main components with a density plot (Figure 3).

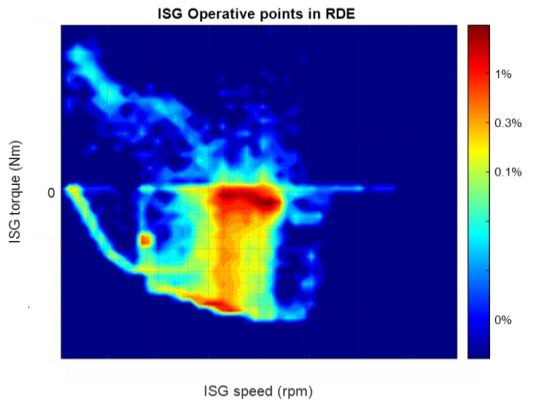

Figure 3. EM2 operative points density map.

The density plot permits visualizing the concentration of data points in a 2D space. This type of visualization is more adequate than the scatter visualization for operative region identification, as the z axis colour shows the frequency of occurrence of a certain point. These types of plots are used to identify the boundaries of validity of the model, as the model will only be correlated within the operative regions that were available in the input dataset. If the predictivity of the model needs to be enhanced to a wider region, the input dataset needs to be increased with input representative input data of that region. For this reason, it is important to generate the models from test that cover a wide operation range, such as the RDE that consists of urban, rural and highway driving and typically excites a wider operative region than WLTP.

The parameters identification is performed with an internal regression tool that has been developed to address the most common cases faced in model parameter identification. Figure 4 shows the identification process of a mathematical formula for a degree of freedom at a certain condition (for example, the operative point of a component in hybrid mode). This process is repeated for the different identified conditions until all the degrees of freedom required to perform a closed-loop simulation are identified.

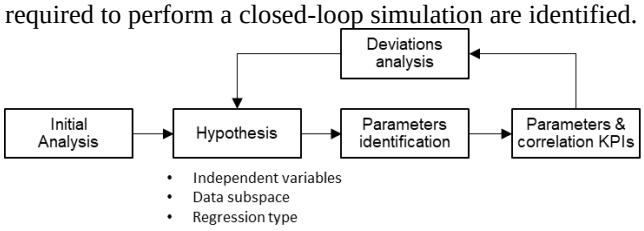

Figure 4. Parameter identification process.

The identification process of a dependent variable starts with a hypothesis of the variables that affect the signal to be simulated based on the laws of physics, experience, and data analysis. For example, from the physical principles we

can expect a motor consumption to be highly related to the output torque and rpm and from experience and data analysis we can expect the torque split strategy to depend on vehicle speed, pedal position, and battery SOC. Afterwards, we select the subspace of data to apply the hypothesis to (for example, when ICE is on) and the type of regression to apply.

The software permits applying Bayesian multivariable regression [5] and linear piecewise fitting [6]. Bayesian regression is a multivariate linear regression that can be used to perform parametrization to a multivariable formula but also to perform a non-linear regression to a certain value by introducing the non-linearity as an additional input signal to the Bayesian process. For example, if we expect the road load to be dependent of the square of the speed, the square of the speed is defined as an additional input to the regression. This multivariable and non-linear correlation is able to cover most of the characterizations representing physical laws and continuous behaviours. The software also performs outlier elimination (Figure 7) following a standard deviation criterion selected by the user (confidence interval of 95% or 99%).

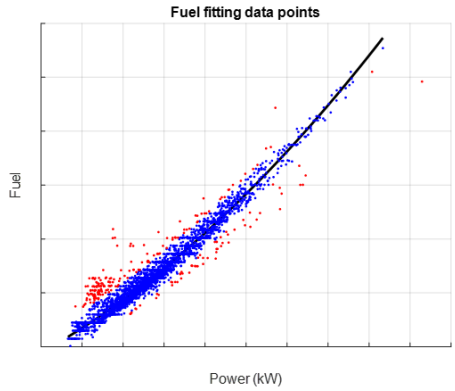

Figure 5. Example of scatter plot for non-linear Bayesian regression with outliers elimination.

The result is a regression curve and the quality KPIs of the regression. As scatter plot does not permit observing the statistical distribution of the points, two alternative plots are generated to better observe the regression: the confidence interval and the density plot (Figure 6)

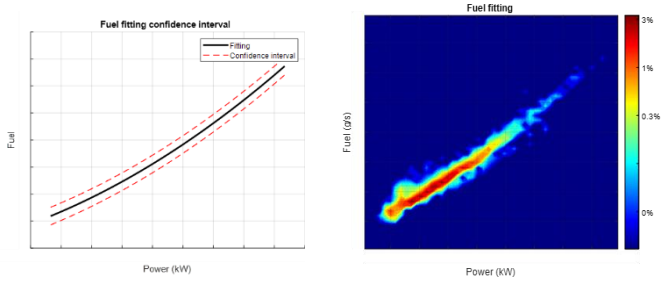

Figure 6. Result of regression as confidence interval (left) and density plot (right).

Components efficiency characterization is usually performed following this Bayesian multivariable approach and applying the Willan's line principle [7]. Depending on the spread of operative points, according to [8] in most cases component speed dependency can be omitted while obtaining good correlation. This does not imply that the efficiency does not depend on speed. It means that the dependency with speed in the restricted operative area observed during the cycle test is not significant for the correlation, limiting thus the application of the model to a restricted operative area. This regression approach is significatively different from the approach when component data is available (in this case, usually 2D, 3D or even 4D maps are used), but has proved to provide very high correlation in the effective operating regions in driving conditions.

The alternative method, Linear Piecewise fitting, is mostly used for strategies identification, as strategies are usually defined as a function of breakpoints and not as a continuous equation. This method is able to automatically perform correlations with discontinuities in the function slope. The method applies an iterative procedure in which both the optimal breakpoint position and the regression within the breakpoints is calculated until the best fit is found (Figure 7). The process also permits to eliminate outliers and plot the confidence interval and density plot as depicted in Figure 6.

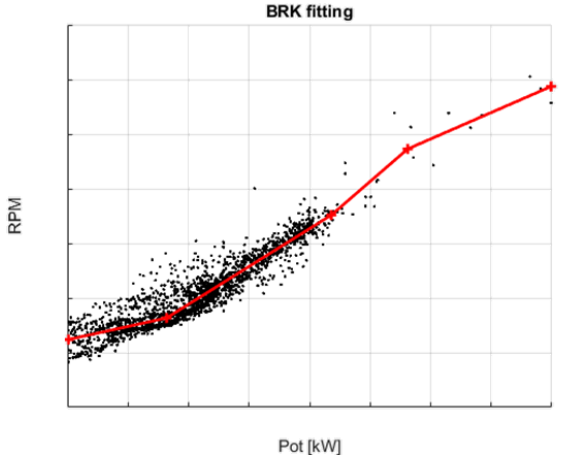

Figure 7. Linear Piecewise regression.

As depicted in the process in Figure 4, the resulting characteristic curves and KPIs of the correlation are evaluated in order to decide if the model identification is correct or the process needs to be repeated with different or more hypothesis. As later explained in Section 2.3, our acceptance criteria for the closed-loop simulation is a correlation of more than 90% for the relevant instantaneous signals. The outcome of this identification activity is just the building blocks to construct the closed-loop model in which the individual model deviations will be amplified. Therefore, the recommendation for this type of regressions is to obtain a correlation higher than 97%. It is understandable that such degree of correlation can only be reached if the data preparation described in Section 3.1 is performed scrupulously.

In this iterative process to improve the individual correlations, a good procedure is to plot the error of the correlation against variables that, even though they are not the main factors of influence, may affect the result such as speed, temperature, pressure, voltage, etc. If the regression result shows a regression function with a variation higher than the confidence interval (95% or 99%), the additional variable should be considered in the hypothesis for multivariate correlation. Figure 8 shows that, for the sample data used for this section, aggregating ICE rpm correction to the consumption model did not increase the accuracy in the operative region represented by this data (Figure 8).

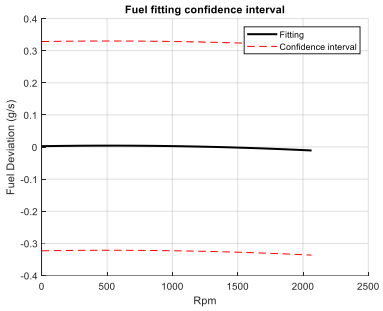

Figure 8. Fuel consumption deviation as a function of rpm.

The process stated in Figure 4 is repeated until the parameter identifications to model all the degrees of freedom and conditions required for the closed loop of the model are within the acceptance criteria.

2.3. MODELLING AND CORRELATION. The modelling process begins with the open-loop modelling of the different components and strategy blocks that will form the complete model. After implementation in the modelling software, the models are excited with test signals and correlated against their expected value. The result should be the same, or very close to, the correlation result obtained during the parameter identification, as the only differences are due to the implementation of the equations in the modelling software.

Afterwards, the most delicate step, is to convert the open-loop model in a closed loop. Gradually, open-loop excitations to the individual models are substituted by closed-loop excitations performed by another model and the connection is validated until the complete model behaves in closed loop.

For hybrid vehicles, it is common that the behaviour during the first integration loops deviates from the expected and even the components operate out of their identified area. This occurs because in the strategy identification process (Section 2.2), the rules that define a control variable value vs another value can be identified by regression, but the limits to a certain strategy are not so clearly identified and need to be tuned in the integration process.

The methodology followed to perform the correlation and iteration of the model identification follows the principle of the [4] correlation framework considering the noise factors (Figure 2).

As stated by [4], for model validation is not enough to provide aggregate end-of-test KPIs (e.g.: total fuel consumption, total regenerated energy, average engine rpm). The risk of using this simplification to evaluate the quality of a model is to perform 2 or more modelling errors (one affecting positively the aggregated result and one negatively) and obtain a good correlation in the aggregated value even though there are significant partial deviations. Figure 9 shows an example in which the final aggregated value correlates well, but not the instantaneous result. This implies that the model consumption is lower in the first part (urban area) and higher at the end (highway driving). Therefore, if we assume that the model is correlated, and we apply it to predict the consumption in different usage profiles [2] or calculate the impact of specific improvements (Section 6) we will induce errors.

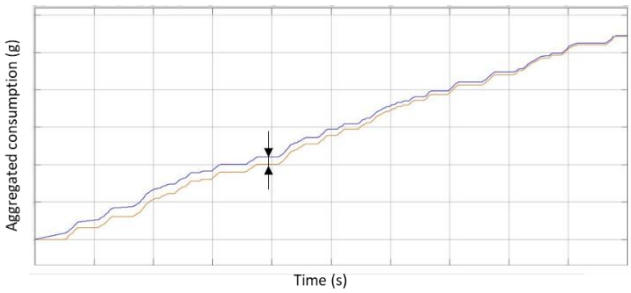

Figure 9. Example of faulty instantaneous correlation.

Models have so many degrees of freedom and noise factors that if only test end aggregated metrics are considered, it is highly probable that a good KPI is obtained from 2 or more deviated characterizations. As proposed by [4], instantaneous correlation of various significant signals is needed to guarantee that the good correlation results are really due to a good predictivity of the model and not due to overfitting of parameters. To measure the level of correlation, the KPI used is the normalized cross-correlation power or NCCP [3]:

$$\mathrm{NCCP} = \frac{\max[\mathrm{R_{xy}}]}{\max[\mathrm{R_{xx}},\mathrm{R_{yy}}]} \tag{2}$$

$$\mathrm{R_{xy}} = \int_0^T x(t) \cdot y(t) dt \tag{3}$$

When using the cross-correlation power all the instantaneous simulation instants affect the correlated result. The signal cross-correlation acceptance KPI in the process is 90%. This acceptance limit, together with a deviation of maximum 5% (desired 2%) in overall aggregated values, consists of a robust method to guarantee model correlation.

However, for hybrid vehicles, we have to assume that for signals dependent on the strategy it is not possible to aim to a 90% of correlation, due to small randomness that affect the application of the strategy and thus the cross-correlation. For example, if the ICE switches on just 5 seconds after the test signal, even though the overall strategy behaviour is correctly covered, that 5 seconds of error will weight significatively in the cross-correlation KPI.

Due to this reason, in hybrid vehicles it is important to define signals that represent well the instantaneous behaviour of physical dependencies (road load, efficiency…) and the strategy scheme, but at the same time are robust enough to not be affected by deviations in which the change of strategies is applied. These types of signals are the instantaneous values of aggregated signals, for example aggregated fuel consumption, aggregated regenerated energy, aggregated battery consumption, etc. The instantaneous correlation guarantees that the model is well correlated and predictable in all the different driving conditions covered in the test, while the aggregation provides robustness against risible strategy deviations. In this type of signal, we can aim at a target correlation higher than 90%. In the rest of instantaneous, and highly variable signals, 80% correlation is a good result in HEVs.

3. MODELLING AND SIMULATION IN USE CASE

The model developed in this paper is based on the hybrid prototype architecture depicted in Figure 10. The vehicle has an electric ISG motor connected to the ICE (EM2) that is used to assist the ICE at stop-start and to recharge the battery when the ICE is on. Additionally, the electric P4 motor in the rear axle (EM1) permits EV driving and torque assist when the ICE is on.

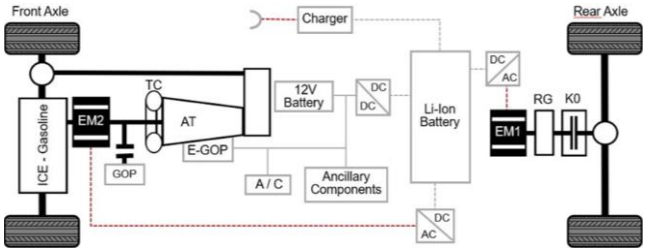

Figure 10. Demonstrator vehicle architecture.

Several validation tests were performed on this prototype vehicle including coast down, WLTP, RDE on chassis dyno and longitudinal performances.

The tests used for vehicle characterization were the coast down test, from which the road load is obtained and the RDE test in chassis dyno. The RDE test was performed on the chassis dyno due to the prototypal state of the demonstrator, but it represents a driving RDE test on open roads performed with the baseline ICE version of the same vehicle. Figure 11 presents an image of the RDE route, and the slope associated with it.

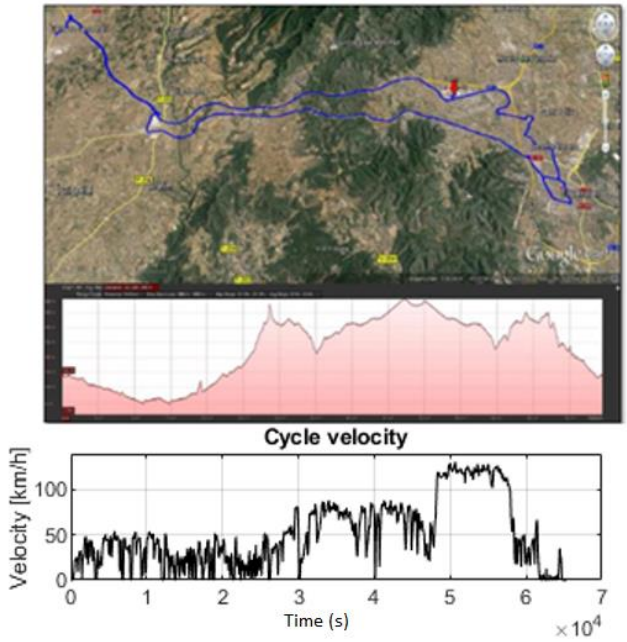

Figure 11. RDE test used for simulation.

This real route recorded was configured in a chassis dyno and performed by an instrumented demonstrator vehicle. The data measured from this vehicle was used to identify all the model's parameters (Section 4), model and correlate (Section 5) and perform improvements impact simulations (Section 6).

4. MODELS IDENTIFICATION

4.1. COMPONENTS

4.1.1. EM2 Efficiency model. The EM2 rotate at the same speed than the ICE motor, thus the ratio between them is 1:1. The operative points distribution of the EM2 is depicted in Figure 3 (Section 2.2). From this figure, it can be observed that the EM2 is used mostly for energy harvesting while ICE is on (negative torque). The positive torque data are instants when the EM2 motor acts as starter to help the ICE motor in cranking moments. This behaviour is sustained only a few seconds.

In this case the electric power and the mechanic power developed by the EM2 are the signals chosen to make the curve fitting for the efficiency. The efficiency modelling follows the principle described in Section 2.2 [8]. The EM2 efficiency correlation for the regeneration region can be observed in Figure 12.

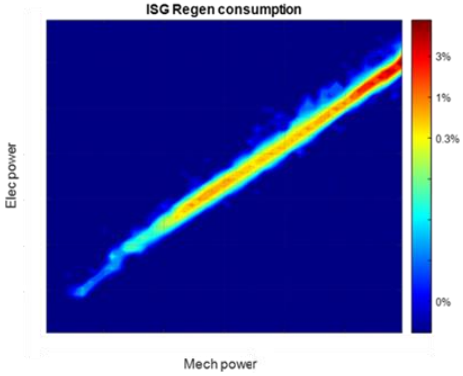

Figure 12. EM2 electric vs mechanic power in regeneration density plot.

It can be observed that the correlation of the two signals is very clear (no data outside the correlation line). The resulting efficiency characterization gives a high level of correlation: 91.8% in traction and a 99.8% in regen. For better evaluation of the level of correlation, Figure 13 shows the predicted vs the measured electric consumption of the regeneration data points.

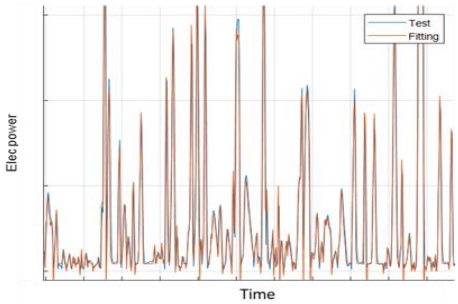

Figure 13. Comparison of EM2 test and calculated electric power.

4.1.2 EM1 Efficiency model. Unlike the ISG motor, whose operation depends on the engine speed, P4 operation is independent from the engine speed and often operates as EV drive with the ICE off. As it is directly connected to the rear axle of the vehicle, when the vehicle is reducing the speed (coasting) or braking, the motor enters regeneration mode while the ICE gearbox is disengaged to reduce motoring losses.

In Figure 14 the operative points of the electric motor EM1 can be observed. As the EM1 is connected through a fixed gear to the wheels, it is observable that its operative range is wider (both in torque and rpm) than the ISG that is subjected to the gearbox reductions.

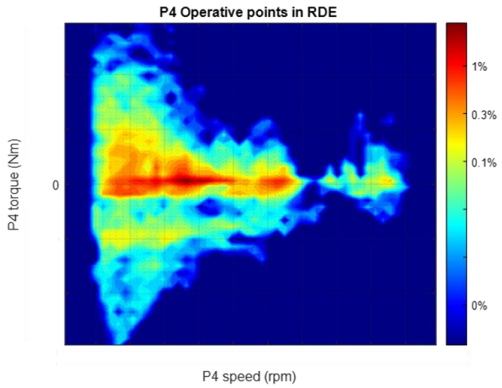

Figure 14. EM1 operative points density map.

Like the EM2 electric motor, both phases, traction and regeneration were treated independently for parameters identification, as the energy flows in opposite directions. Figure 15 shows the electric power vs mechanical power of EM1 in regeneration and traction mode respectively.

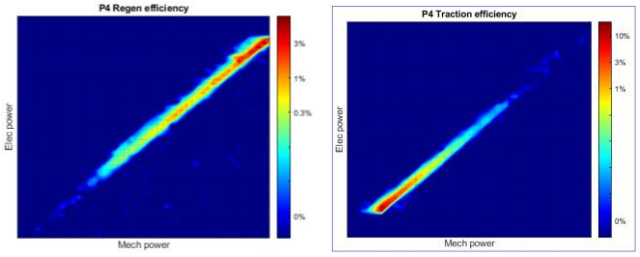

Figure 15. EM1 electric vs mechanic power in regeneration (left) and traction (right) density plot.

As in the case of the EM2 electric motor, the correlation of the efficiency model for traction and regeneration in motor EM1 has a high degree of accuracy: 98.4% and 98.7% respectively. As an example, Figure 16 presents the electric power comparison between the test data and the calculated values for the traction part. The regeneration part is very similar with a high level of correlation too.

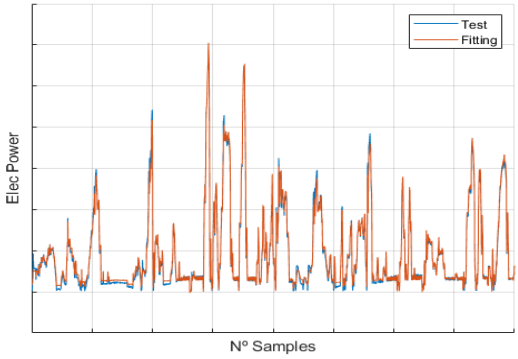

Figure 16. Comparison of EM2 test and calculated electric power.

4.1.3. Battery model. The battery model has to model three different behaviours to reach the adequate level to correlate with the test signals:

- SOC variation with discharge and charge currents.
- OCV (Open Circuit Voltage) as a function of SOC.
- Equivalent internal resistance.

In this case, the battery capacity was known data from the component specification. This data, and the instantaneous SOC measurement were used to analyse the current measurements (by Hioki and by CAN) and to identify the offsets. Offsets are commonly found in current signals as explained in Section 2.1, and even though small, the aggregated offset during a long driving cycle (RDE typically lasts around 2h) is a value completely out of the acceptance criteria range of the correlation and that affects the correlation of the rest of the signals. Therefore, in this case, the regression process was used to identify the correction factors for the measurements from known component data and trusted measurements. After offsets correction, SOC measurement vs SOC calculation from measured currents is consistent, as shown in Figure 17. The correlation value obtained for this, was 96%.

$$SOC(t) = SOC(t_0) + \int \frac{I}{3600 \cdot Capacity(Ah)} dt \quad (4)$$

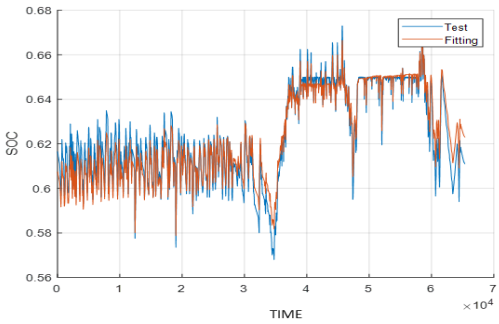

Figure 17. SOC comparison between test and regression model.

Battery OCV and internal resistance are obtained by a multivariable non-linear regression of voltage vs SOC and discharge current. The relation of OCV with SOC is non-linear but is usually well approximated by a polynomic function of the SOC. Adding the discharge current to the multivariable regression makes it possible to identify the voltage drop due to the Joule losses as shown in Figure 18. The equivalent resistance of the battery is then the slope of the resulting linear regression.

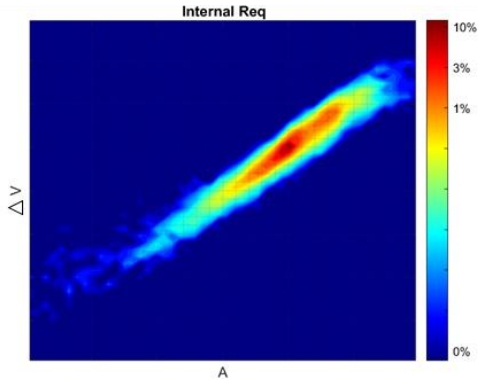

Figure 18. Equivalent internal resistance regression.

As the multivariate regression applies the voltage drop correction as a function of discharge current, the resulting correlation of Voltage vs SOC represents the estimated voltage at zero current. The behaviour of the battery voltage is then approximated by the following function:

$$V = f(SOC) + R_{eq} \cdot I \quad (5)$$

The polarization curves for this model obtained from the regression are presented in Figure 19. These curves indicate how the voltage of the battery changes with the SOC, at different charge and discharge currents. As discussed in Section 2.2, the validity of the regression model is within the range of data observed during the experimental activity, in this case between 56% and 68% SOC. If a model of different SOC levels was needed, the testing campaign would need to be completed with high SOC and low SOC testing activities.

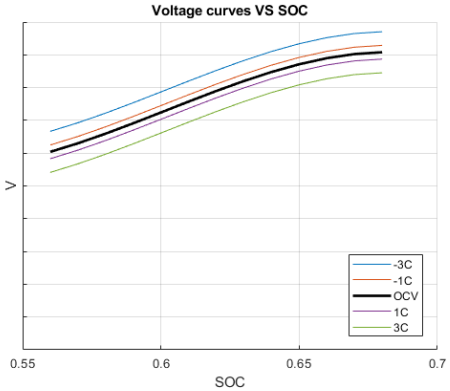

Figure 19. Battery model polarization curves.

Figure 20 shows the correlation of the measured and the calculated voltage calculated from the polarization curves. The correlation value obtained is 99.9%.

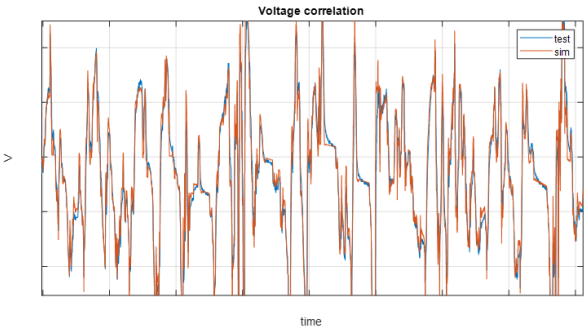

Figure 20. Voltage comparison between test and regression model.

4.1.4. ICE consumption model. As with the electric motors, the process applied to identify the ICE consumption model follows the process described in [8]. The density map of the torque and speed of the ICE from the test data show the operative points of the engine during the RDE cycle (Figure 21). It can be observed, thanks to the gear strategy used in the demonstrator, that the ICE motor is able to work in a very narrow band of speed making it possible to neglect the influence of speed in consumption in this tight region. The hybridization with the EM1 and EM2 also make it possible to increase the torque of the operative points, locating them in the high efficiency regions of the ICE for longer periods than the baseline vehicle.

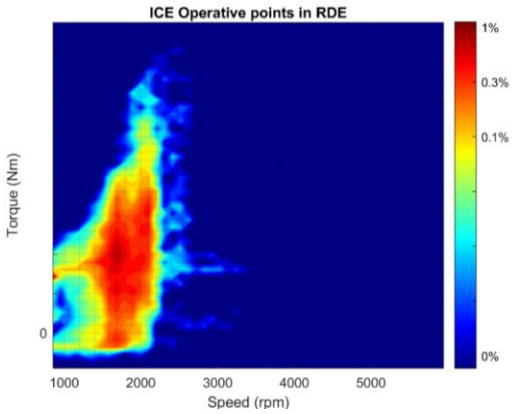

Figure 21. ICE density map of operative points.

The signals that provided higher correlation to make the regression of the fuel consumption were the instantaneous consumption in g/s vs ICE mechanical power and coolant temperature. Even though according to [8] fumep (g/rev) vs torque should be more correlated due to the Willan's line principle, in practice dividing the consumption by the rpm produces noise that decreases the correlation. Figure 22 shows the regression of fuel consumption vs mechanical power.

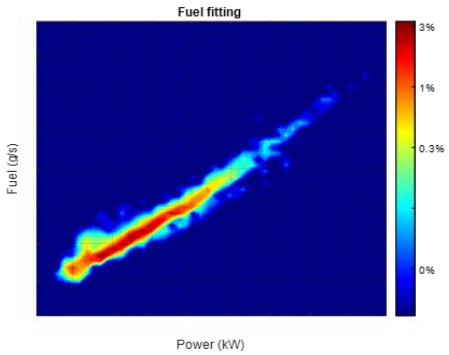

Figure 22. Fuel consumption regression with the mechanical power.

The resulting equation for the modelling is as follows, where C represents a constant value. The temperature also has an impact in fuel consumption and thus, at low temperatures, a correction is performed:

$$\text{Consumption (g/s)} = C + f(P_{mech}) + f(T) \qquad (6)$$

Using the curve regression and the low temperature correction, the resulting level of correlation is 98.9%. To show the validation of this model, an image of the fuel consumption comparison between the test data and the calculation mode is presented in Figure 23.

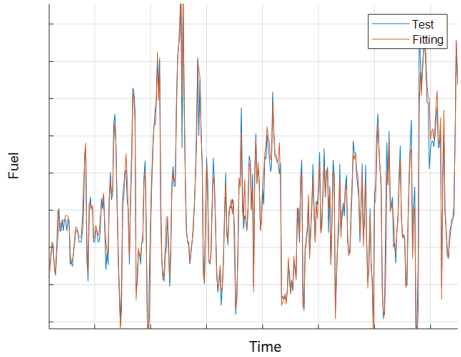

Figure 23. Comparison between test and calculated fuel consumption.

At this point the regression models of the EM1, EM2, ICE and battery were modelled and validated. The rest of the models (transmission, rotational inertias, auxiliaries consumption…) were also obtained from analysis of the test results following a similar process, but for the road load it was calculated following the WLTP test procedure [9].

Next paragraphs show the identification of the different modes of operation and the strategy of the torque split.

4.2. OPERATION STRATEGIES

4.2.1. States strategy. Strategy identification was performed analysing the test data recorded and dividing the test time in different frames. Each of the frames are related with the different operation modes of the demonstrator. After analysing the data, 3 main modes were identified:

- Only ICE mode: only the ICE provides traction to the wheels. During this mode, the ISG may recharge the battery.
- Hybrid mode: the ICE and ERAD provide traction to the wheel simultaneously, the ISG can recharge the battery if needed.
- EV mode: only the ERAD motor is providing traction and/or retention to the wheel.

Figure 24 shows the full EV mode and when the ICE is on, consuming fuel. The hybrid mode and regeneration phases are not shown for better readability. It can be observed that the operative strategy permits full EV driving, but the full EV driving periods are short.

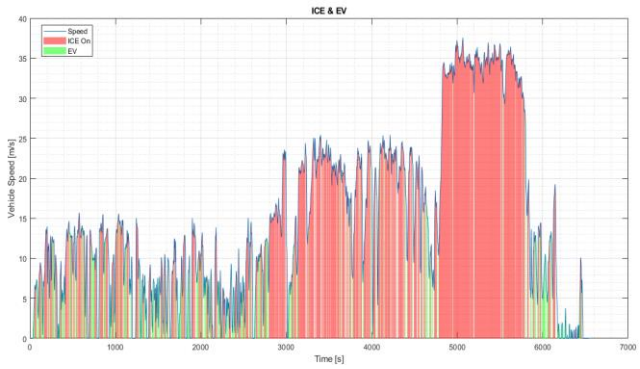

Figure 24. ICE on and EV mode phases during the test.

The strategy permits two forms of recharging the battery:

- ISG: ISG performs energy harvesting when ICE is on, making the ICE work at higher torque and thus higher efficiency.
- ERAD: regeneration when the vehicle is coasting or braking.

Energy harvesting in this demonstrator has a particularity, harvesting by the ISG also occurs in HEV mode while ERAD is providing traction. This means that part of the mechanical energy produced by the ICE is converted into electrical energy through the ISG and then to mechanical energy again by the ERAD motor. This behaviour only occurs occasionally and probably, ERAD contribution has a positive impact on driving dynamics, but it is negative for the overall efficiency of the demonstrator vehicle.

The main signals responsible for changing the operation mode were identified by analysis of the data and splitting the data in clusters according to operation modes. Those signals were SOC, velocity and accelerator position.

Focusing on those signals and the moments when the modes change, a states strategy was developed. Figure 25 shows the states diagram that summarizes the identified control logic for the different modes of operation.

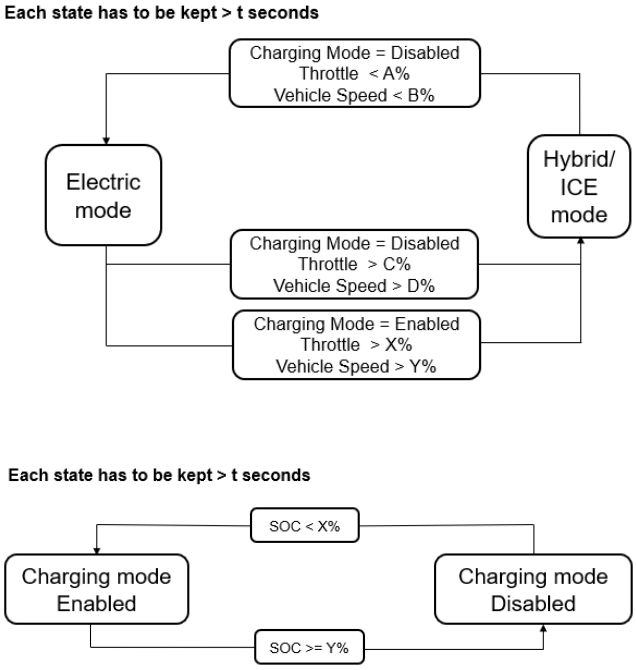

Figure 25. Vehicle traction mode transition strategy (top) and SOC hysteresis (bottom)

The transition from electric mode to HEV or ICE mode is determined by cycle demand (pedal and velocity) but also as a function of a hysteresis of the SOC. When the SOC is lower than a certain threshold, a charging mode, which enhances energy harvesting, is activated until the SOC reaches a target value. Afterwards, EV driving is prioritized.

4.2.2. Torque split strategy. The torque split strategy is also necessary to develop the complete vehicle simulation model. Within a certain state, the strategy distributes the power requirement from the driver to follow the speed target between each of the traction units: ICE, ISG and ERAD.

Also, in this case the strategy is implemented by analysing the test data signals of the torque for the different sources and identifying rules by repetitively applying filters and regressions. This is a complicated process because the torque interaction between the motors is dependent on the operation mode in traction and regeneration. Data filters are used to performed piecewise correlations for each of the driving modes.

The torque split strategy is divided into two main calculation blocks. One of them manages the level of harvesting of the ISG and the corresponding torque shift of the ICE while the other manages the torque boost provided by the ERAD motor and the regeneration limits during braking.

A similar identification process was applied to identify the gear shifting strategy and the pedal calibration strategy.

5. MODEL IMPLEMENTATION AND CORRELATION

5.1. OPEN LOOP. The first step of model creation is open-loop modelling in which all the models are generated individually in open loop and excited with test data. The objective is to make a step-by-step implementation and guarantee the correlation of each step in order to prevent complex problem-solving issues. At this stage, all regression models are modelled in the selected simulation software and validated against the test data. The inputs for the open-loop model were retrieved from the recorded test signals, and the outputs simulated were compared to the same equivalent signals recorded from the test. The correlation obtained should be the same as the regression, the only deviations being due to the model implementation. This step permits solving model implementation deviations before the deviations affect the result in closed loop.

All the regression models developed have the possibility to be introduced in various simulation software for powertrain simulation. In this case to validate the complete vehicle model in open loop, the selected software was Simcenter Amesim.

Then the next step is to progressively integrate the models in a complete vehicle model by feeding a component model with the calculated signals from other models until the only signals that remain in open loop are the strategy. Figure 26 shows the demonstrator plant vehicle model in open loop in Simcenter Amesim.

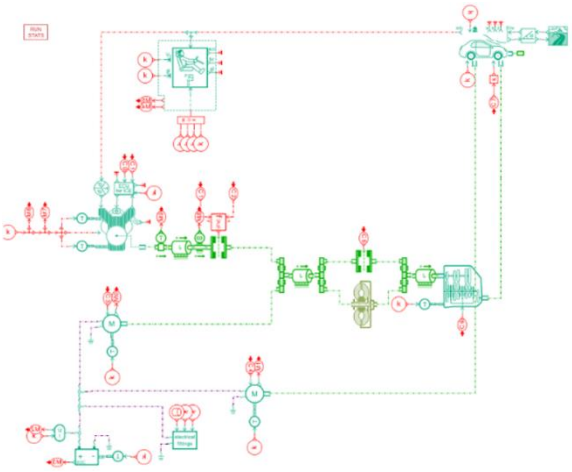

Figure 26. Demonstrator vehicle model in open loop

The open-loop implementation provided good results. The main variable of analysis, the instantaneous aggregated fuel consumption, provided 99.8% correlation between the demonstrator vehicle and the open-loop vehicle plant model.

The following step was to develop the models for the control strategies in open loop: states strategies, torque split strategy, gear shifting, and pedal calibration as shown in Figure 27. The selected software for the strategies implementation was Matlab/Simulink.

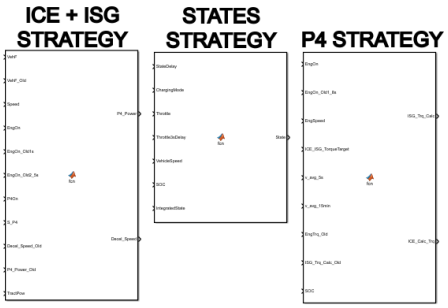

Figure 27. States and torque split controls in Simulink.

5.2. CLOSED LOOP. The closed-loop model is implemented by connecting the open-loop component models with the open loop strategy models in Simulink in a co-simulation environment. Both software applications have blocks (Figure 28) to interact between them. The simulation flows as follows:

1. Both software applications initialize the models.
2. The Amesim model executes a time step in the simulation and sends the required signals for the strategies to the Simulink interface block.
3. The Simulink model receives the signals, executes the time step in the simulation and sends the strategies output signals to the Amesim block interface.
4. Amesim model receives the signals from Simulink and ends the rest of the calculations for the step time.

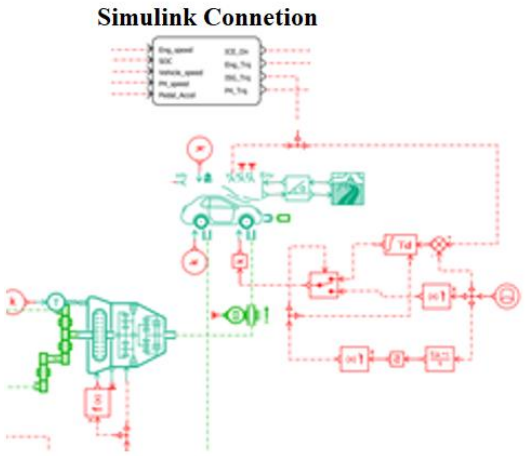

Figure 28a. Amesim block to connect with Simulink.

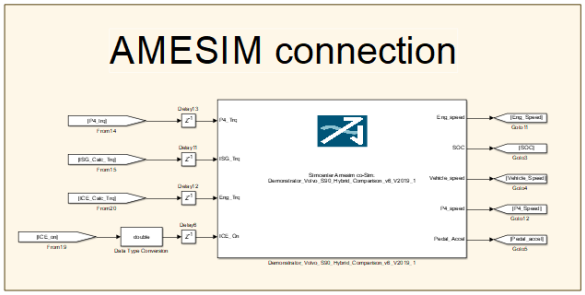

Figure 28b. Simulink block to connect with Amesim.

The strategies extracted through regression of the test data recorded are a first approach to the final strategy. Once the complete vehicle model in closed loop was implemented in the software, including the strategies, it was necessary to iterate in several loops for the tuning of the strategy, specially to define boundaries that are complex to identify just by analysing the test data, but make the model deviate in closed loop. With the tuning, new conditions were implemented to change one mode to the other and new limits were established until the required correlation was reached. The same regression tools used for the first identification are used for tuning the strategies in closed loop with further conditions.

5.3. SIMULATION VALIDATION. The last step is the validation of the whole model comparing the closed-loop model signals with the test signals with the methodology described in Section 2.3. This methodology guarantees high confidence on the correlation of the model and ensures that the correlation is not causal, as a high level of correlation is checked for several signals at every instant of simulation. The main KPI for the correlation is the accumulated fuel consumption, as it is also the KPI that will be used to analyse the savings of the vehicle. After performing a complete simulation, the comparison between the accumulated fuels is presented in Figure 29.

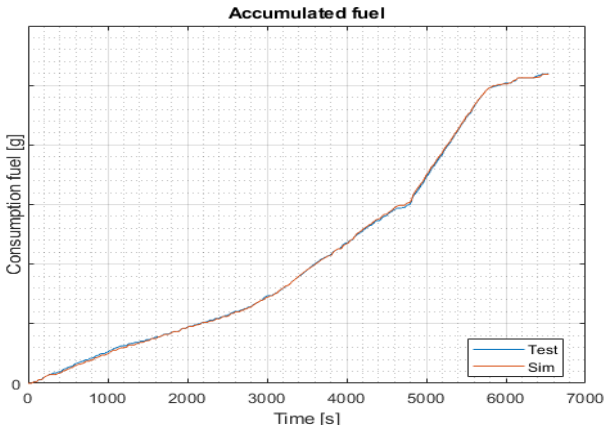

Figure 29. Accumulated fuel comparison between simulation and test data.

The closed-loop model developed correlates very tightly during all the simulation time, even though the entire model was built from analysis of test data. This is a very good indicator of the validation for the closed-loop model and the predictivity of the model.

A closer look at other signals, proves that the correlation of the fuel consumption is not casual, it is due to good correlation of the behaviour of the different strategies and components.

The strategy defines the instants when the ICE must operate and the engaged gear. Thus, the speed of the ICE in simulation compared with the ICE in the test is another relevant validation indicator, especially for the strategy. For readability, Figure 30 shows only a fragment of the complete simulation time. The speed in both cases is very similar as well as the instants of the ICE operation.

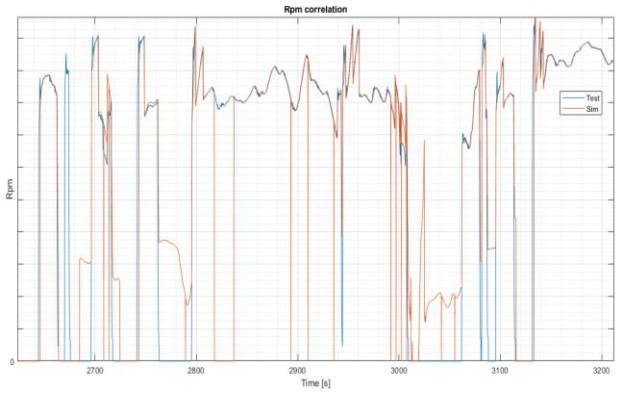

Figure 30. ICE rpm comparison between simulation and test

Instant fuel consumption correlation is also good proof of correlation, as good correlation also proves correct identification of the torque split strategy and the ICE efficiency map (Figure 31).

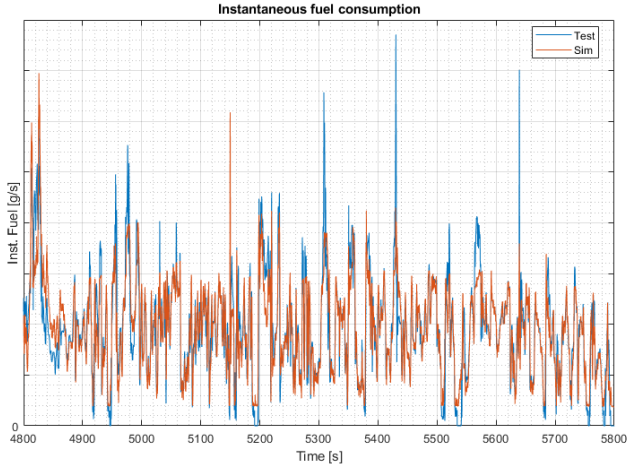

Figure 31. ICE consumption comparison between test and simulation.

The signal probably most affected by the strategy is the instantaneous battery SOC as it depends on the auxiliaries consumption and the traction and regeneration power of each motor. The strategy of the demonstrator vehicle shows a clear charge sustaining strategy that is well captured by the model. The developed strategy acts in the same form, always

maintaining the SOC inside a narrow range of values. A deep look at Figure 32 makes it possible to observe that in some instants, there are small SOC deviations because of the ICE turning on and off some seconds before or after the test, but the strategy is captured very well, and the model recharges the battery in the same instants as in the RDE.

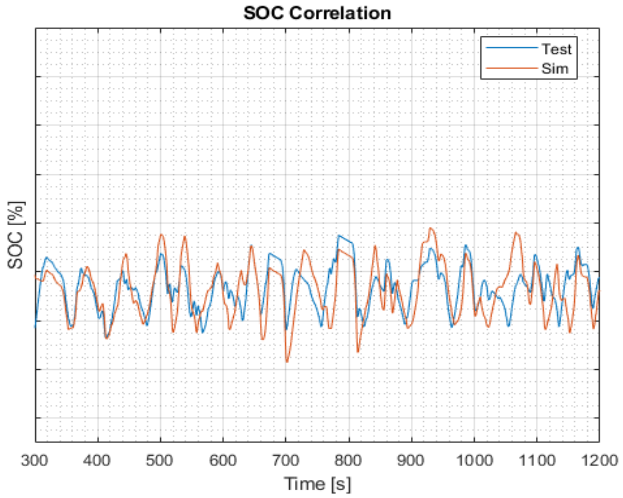

Figure 32. Battery SOC comparison between test and simulation

The last signals presented here in order to show the validation process are the mechanical power delivered by the ERAD motor in the test and the simulation. The comparison between the test data and the simulation results are shown in Figure 33. The ERAD power is another indicator of the strategy functionality because the strategy has to select the correct mode (hybrid or full electric) and the torque split.

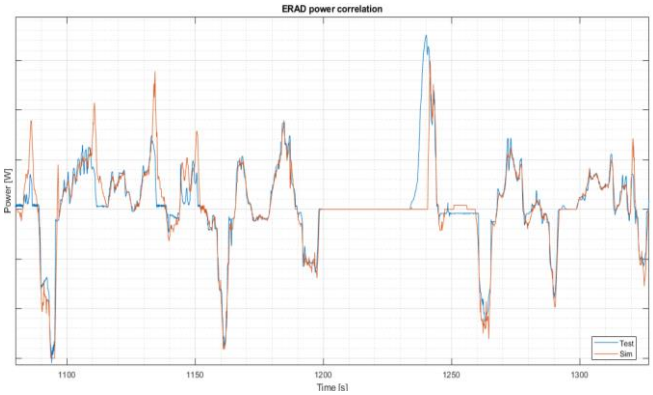

Figure 33. ERAD electrical power validation.

Table 1 presents the summary of the main correlation metrics as described in Section 2.3. The open-loop results show the KPIs of the individual components performance (98-99%) and the closed loop shows the KPIs of complete model. It can be observed that the correlation when component parameters identification has to be very high in order to guarantee high correlation also in closed loop. It can also be observed that, in closed loop, cumulated metrics (SOC, ICE energy, ISG energy, ERAD energy) even though calculated at each time step, are more robust because they are not greatly affected by slight delays in the strategies changing modes. On the other hand, instant metrics such as rpm and instant consumption are more sensitive, even though correlation results are very good.

Table 1. Correlation values summary.

Open loop	
ISG instant electric regen	99.8%
ERAD instant electric traction	98.4%
ERAD instant electric regen	98.7%
Battery SOC	99.9%
ICE instant consumption	98.9%
Closed loop	
Battery SOC	99.8%
ICE cumulated consumption	99.8%
ISG cumulated energy	93.4%
ERAD cumulated energy	89.2%
ICE rpm	83.7%
ICE instant consumption	86.5%

6. SIMULATION RESULTS

This section presents the exploitation of the correlated and validated model to simulate the impact of varying vehicle parameters and strategies. This simulation platform for hybrid vehicles can be connected to a simulation manager to plan the execution of multiple simulation cases. This makes it possible to perform automatic simulations changing parameters of the model for each case and to analyse the impact on the vehicle behaviour, in this case, the vehicle consumption.

For proper evaluation of the impact of different parameters in consumption, it is important to guarantee that all the simulations are performed in comparable conditions. All the simulations performed start with the same initial SOC but end at different SOC because it depends on the cycle demand. This difference of end SOC between simulations affects the fuel consumption result, as the ICE has to provide more or less energy depending on the case, masking the effect of the parameter under analysis. In order to prevent this undesired impact, the difference of battery stored energy at the end of the simulation is converted into an addition or a subtraction of the equivalent fuel consumption. This

correction is performed with a formula based on the RCB CO_2 correction [10]:

$$CO_2\ corr = \frac{(\int I_{bat} \cdot V_{bat} \cdot dt) \cdot WillansFcator}{ISG_{Eff} \cdot Distance} \quad (7)$$

Where I_{bat} and V_{bat} are the current and voltage of the battery, the distance is the total distance of the cycle, the fuel specific Willan's Factor of the engine [11] and. ISG_{Eff} corresponds to the ISG motor average efficiency in harvesting. The Willan's Factor value depends on the type of fuel and engine, in this case petrol E10 and turbo engine.

This correction permits to obtain a comparable fuel consumption KPI among different simulations.

In order to analyse the potential of consumption reduction, first a sensitivity analysis was performed to identify the impact of different possible reductions. The sensitivity was calculated by evaluating the impact of varying the following parameters:

- Reduction of vehicle weight. In this case, vehicle weight also affects the rolling resistance
- Reduction of aerodynamic drag
- Reduction of rolling resistance
- Reduction of auxiliaries consumption
- Increase in the amount of ISG harvesting when ICE on
- Reduction of battery losses due to internal resistance
- Increase of the maximum ERAD braking regeneration

Each of these parameters was varied 10% sequentially and the sensitivity of these factors in consumption was calculated applying the following formula:

$$Sensitivity = \frac{\Delta Consumption/Consumption}{abs(\Delta Parameter)/Parameter} \quad (8)$$

The sensitivity metric shows the hypothetical consumption reduction if the parameter was modified 100%. This value is just a metric of the impact of each parameter to identify the most relevant ones and does not guarantee that the linearity of the impact would be preserved up to a 100% variation.

Figure 34 shows the result of the sensitivity analysis. It can be observed that the highest impact is due to the parameters that affect the energy demand of the route (weight, rolling resistance, aerodynamic and auxiliaries consumption). Weight sensitivity has the highest impact, but it can be observed that the marginal impact of just modifying the mass (by comparing to rolling resistance variation) is small, just 7%. This occurs due to the regeneration capacity of the hybrid part of the powertrain. Weight variation has lower impact than ICE vehicles because most the energy invested in inertia during accelerations is recovered in decelerations (coasting or braking), the only losses are due to motors and transmission efficiency and the infrequent use of the hydraulic brake.

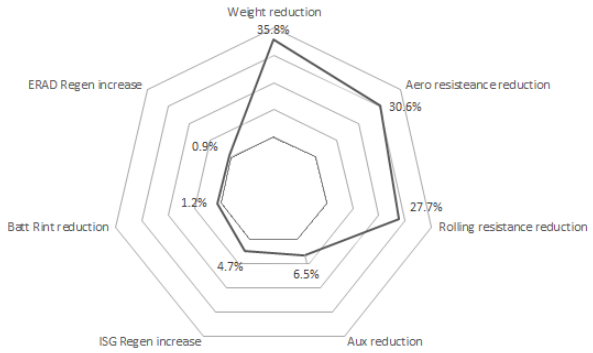

Figure 34. Fuel consumption sensitivity analysis results.

In general, the sensitivity value corresponding to the aerodynamic and rolling resistance is similar to the one obtained in an ICE vehicle and also has a high impact due to its effect on energy demand.

The auxiliaries power has a reasonable impact on fuel consumption with a 6.5% of sensitivity. Followed by the ISG regeneration capacity sensitivity with a 4.7%, showing that an increase of ISG torque would improve the average efficiency of the ICE and reduce consumption. This low value is due to the architecture of the demonstrator vehicle.

The impact of reducing the internal resistance of the battery is very low, with a sensitivity of 1.2% in fuel consumption. The impact is directly related with the current flowing in and out of the battery. Due to the high voltage of the battery, the current needed to develop the same power is lower than for a battery with a voltage lower than 395V. This is because, in this case, reducing the internal resistance does not affect fuel consumption much. In a fully electric vehicle with the same internal resistance, the impact would be higher due to more energy flowing out of the battery to provide traction.

Even though regeneration is crucial for fuel consumption reduction in hybrid vehicles, ERAD regeneration increase sensitivity, is the lowest in this study with apparently no impact on fuel consumption. But the reason for this is that the regeneration strategy is already very optimized and, in this cycle, almost all the coast and braking energies are regenerated thanks to the strategy and the sizing of the ERAD motor. If the regeneration torque of the ERAD is raised 10%, there is no effect on the regenerating energy because with the baseline torque regeneration value, the motor was regenerating almost everything. If the mission profile were changed to a more aggressive cycle with stronger deceleration values, the fuel consumption sensitivity of raising the regenerative torque in the ERAD would be higher.

As a conclusion from this analysis, working on improvements regarding the weight, aerodynamic and rolling resistance will have a significant impact on fuel consumption. But most of the time improving these aspects, like aerodynamic resistance, will have a high cost and or low

improvement margin. Improving other characteristics with a moderate impact on fuel consumption could on the other hand be a more feasible investment with good results, i.e. reducing the auxiliaries consumption using more efficient components and improving the isolation of the vehicle cabin. This study on the impacts could be further developed with a detailed analysis of the different contributions to the coast down [12] by splitting the drag into aerodynamic, rolling resistance, brake pads drag, wheel hub drag, and drivetrain drag. The last ones, despite having a small impact on consumption, sometimes permit high improvements potential up to 50-100% providing an overall impact on the vehicle consumption up to 4% when improved.

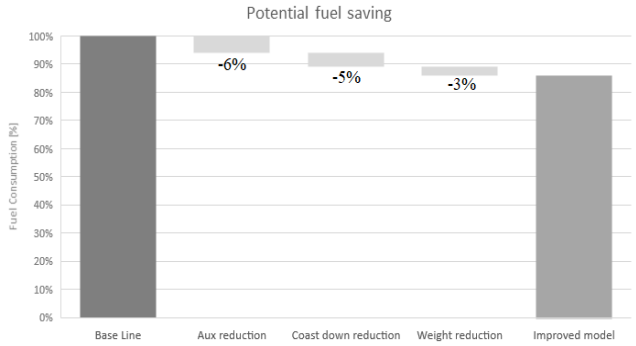

Figure 35. Potential fuel saving with improvements with vehicle improvements

As a sample of the methodology, a set of reasonable improvements in the auxiliaries, road load (aero and rolling resistance) and the weight have been simulated in order to see potential saving in fuel that can be achieved. The result of the simulations gives a 14% fuel saving with the improvements simulated within a reasonable range. The amount of fuel saved with each improvement is presented in Figure 35. It can be observed that even though the sensitivity of the auxiliaries is low, the high possibility of improvement permits a reduction of the same amount of the road load that in this case has less margin to be optimized.

Another advantage of the simulation platform and the closed loop model development is the simulation for different speed cycles or user-specific mission profiles [2]. As an example of the potential, in this case we also simulated the impact of a 10% speed reduction, obtaining a 12% reduction in energy consumption (Figure 36). The study of the driving behaviour impact will be extended in further studies [2,13]. However, this sensitivity simulation already outlines that the role of drivers in reducing global CO2 emissions by implementing eco-friendly driving practices is as relevant as the role of vehicle manufacturers through technology optimization. Encouraging all of us, as drivers, to take an active part in CO2 reduction by adopting efficient driving styles.

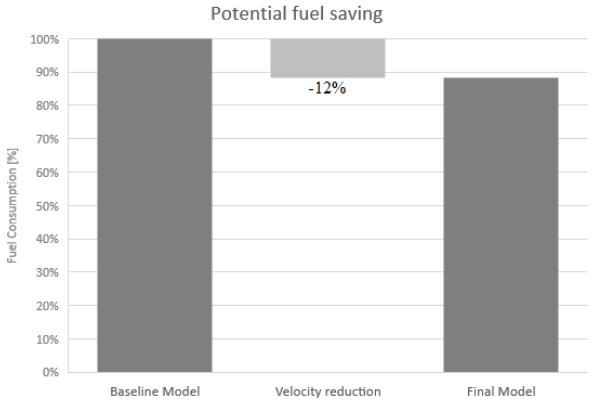

Figure 36. Potential fuel saving with speed reduction

7. SUMMARY

A simulation platform and a model of a hybrid vehicle has been developed within the scope of the European founded ADVICE project in which various demonstrator vehicles were hybridized and validated. The recorded data of a real driving test was processed following an analysis methodology developed to generate reliable models only from experimental data. Analysing the test data recorded from the demonstrator vehicle, the signals responsible for the different modes of operation (only ICE, hybrid and full electric) and strategies (torque split between the motors, gear change strategy, etc.) were studied and identified with very accurate correlation results for the individual models.

The different strategies of the demonstrator vehicle are implemented in the complete model and this simulation in closed loop is validated against the test data of the demonstrator vehicle, obtaining a high correlation value in the fuel consumption. A model test correlation framework was followed to guarantee the correct performance of the component models. This framework makes it possible to systematically guarantee that the complete vehicle model predictivity is correct and prevents random correlations, by validating the correlation metrics of several relevant signals both at end-of-test and at instantaneous results. The correlation results obtained were very high, proving that this methodology is trustworthy to develop simulation frameworks exclusively from test data.

This simulation platform was used to calculate the impact of improving various component characteristics and strategies on fuel consumption as well as simulating the impact of speed reduction on fuel consumption.

This study demonstrates that it is possible to generate reliable consumption models exclusively from dynamic test cycle data and coastdown tests, without the need for additional specific testing if a proven methodology is followed scrupulously. The result of this study shows that this methodology has the potential to boost the outcome of the experimental activities, permitting identification of relevant parameters and strategies, simulating the impact of potential improvements and even new driving cycles.

REFERENCES

[1] http://www.iesta.at/advice/

[2] M. Roche, R.Salat, D.Sabria, F. J. Diaz, P. Cano, "Virtual Modelling of Real- Driving Conditions for Early Evaluation and Validation of Vehicles Design", F2021-ADM-130

[3] Papoulis, A. The Fourier Integral and Its Applications. New York: McGraw-Hill, pp. 244–245 and 252-253, 1962

[4] Yan Meng, Mar Jennings, Poyu Tsou, David Brigham, Douglas Bell and Ciro Soto "Test Correlation Framework for Hybrid Electric Vehicle System Model", doi:10.4271/2011-01-0881

[5] Box, G. E. P.; Tiao, G. C. (1973). "8". Bayesian Inference in Statistical Analysis. Wiley. ISBN 0-471-57428-7.

[6] Muggeo, V. M. R. (2003). "Estimating regression models with unknown break-points". Statistics in Medicine. 22 (19): 3055–3071. doi:10.1002/sim.1545. PMID 12973787.

[7] Pachernegg, S., "A Closer Look at the Willans-Line," SAE Technical Paper 690182, 1969, https://doi.org/10.4271/690182

[8] Phlips, P., "Analytic Engine and Transmission Models for Vehicle Fuel Consumption Estimation," SAE Int. J. Fuels Lubr. 8(2):423-440, 2015, https://doi.org/10.4271/2015-01-0981.

[9] Worldwide Harmonised Light Vehicles Test Procedure

[10] D. Tsokolis a, S. Tsiakmakis b, A. Dimaratos a, G. Fontaras P. Pistikopoulos a, B. Ciuffo b, Z. Samaras "Fuel consumption and CO2 emissions of passenger cars over the New Worldwide Harmonized Test Protocol", doi:10.1016/2016-07-091

[11] ACEA WLTP-08-06 WTLP Open Issue Phase 1B

[12] X. Urgell, "Combined methodology for determination of running resistance split up", F2016-AVCE-004

[13] M. Roche, D.Sabria, P. Cano, D. A. Ruiz, "Objective Impact Evaluation of Predictive Eco-Driving Optimization Algorithm in Traffic Simulation Environment", F2021-ACM-122

ACKNOWLEDGEMENTS

This project received funding from the European Union's (EU) Horizon 2020 Research and innovation program under grant agreement N 724095.